Available online at www.sciencedirect.com
SCIENCE DIRECT®
Chemical Physics 302 (2004) 243–249
Chemical Physics
www.elsevier.com/locate/chemphys

Linestrength of the visible oxygen atmospheric transition

G. Di Stefano *

Istituto di Metodologie Inorganiche e dei Plasmi, C.N.R., P.O. Box 10, 00016, Monterotondo Scalo, Roma, Italy

Received 20 January 2004; accepted 7 April 2004
Available online 10 May 2004

Abstract

The linestrength distribution among branches of molecular oxygen strongest atmospheric transition, $b^1\Sigma_g^+$ $v' = 0$–$X^3\Sigma_g^-$ $v'' = 0$ also known as the A band, is reported as deduced from experiment. Essential deviations from the expected structure, in terms of commonly used theoretical expressions for species in the Hund (b) case, are put in evidence. New expressions, obtained by a distinction between intermediate (a)–(b) and full (b) Hund cases, lead to a satisfactory agreement with the experiment.

Keywords: Linestrength; Gas; Diatomics

1. Introduction

The oxygen molecule has, for many years, involved multidirectional interests because of its very special place in all questions related to life and environment. Its chemical and photochemical behavior, for example, is a recurring subject in investigations both on global models of atmospheric processes [1,2] and, due to increased aerospace activity, on questions of a strictly technological nature.

In fact, state-to-state data on molecular oxygen [3] are of a great interest for diverse applications. In this context, great efforts have been made for the evaluation of line parameters of atmospheric transitions, and an extended and highly reliable report of the O_2 ($b^1\Sigma_g^+$–$X^3\Sigma_g^-$) system has been achieved by Babcock and Herzberg [4] in 1948. Here, line positions of the most intense bands (580–770 nm) were deduced by comparing absorptions in the open air (up to 100 km) and the laboratory (30 m). These data are still a widely used reference for studies, also in emission [5], on positional line parameters.

However, data on the dual aspect, with respect to position, of intensity line parameters have long been lacking in spite of serious attempts [6]. In the last few decades, on the other hand, linestrengths of oxygen's A band have been reported, though to our knowledge only evaluated from absorption data [7–9]. Their functional dependence on rotations has been deduced [7,9], or presumed [8], to substantially agree with well-known theoretical expressions [10]. The strength of rotational lines, actually, is a highly sensitive factor (identical in Einstein absorption and spontaneous emission coefficients) likely to play a "fingerprint" role, in particular for diatomics. A special interest in this area should be addressed to weak transitions, where the structure of the linestrength distribution may shed light on spin dynamics and the underlying mixing of states. In this study, the linestrength distribution among A band branches is obtained from the emission intensity of rotational lines.

The basic difficulty of the intensity approach to metastable states obviously lies in the weakness of transitions. The oxygen molecule too is a relatively weak species as a light absorber and emitter [3,11], i.e., photon exchanges between its lowest states and the field are strongly hindered by spin and orbital selection rules [12]. Nonetheless, abundance makes the O_2 ($b^1\Sigma_g^+ \rightarrow X^3\Sigma_g^-$) radiation to be among most intense items of terrestrial atmosphere [13], with the A band featuring dayglows [14], nightglows [15] and aurorae [16] by different channels. The b–X transition is also remarkable in a more general sense, as part of complex oxygen energetic and chemical balancings [17–20].

* Tel.: +39-06-90672215; fax: +39-06-90672238.
E-mail address: giorgio.distefano@imip.cnr.it (G. Di Stefano).

0301-0104/$ - see front matter © 2004 Elsevier B.V. All rights reserved.
doi:10.1016/j.chemphys.2004.04.010

According to above, the O_2 ($b^1\Sigma_g^+$ $v' = 0$–$X^3\Sigma_g^-$ $v'' = 0$) band is acknowledged the best intermediate for atmospheric spectroscopy [7–9], as for example in remote sensing by the laser absorption technique (lidar [21]). In other words, atmospheric pressure, temperature, density, etc. can be monitored accurately according to A band line parameters, which are of an isolated-particle [22] nature, not depending on ambient. Aeronomic spectroscopy, satellite measurements of cloud tops height and weather observation are among the typical goals of these activities ([7–9, and references therein]). Therefore, apart from such questions as the spin dynamics in oxygen (strictly an object of this study), a detailed knowledge of the A band structure should be relevant also for monitoring techniques.

In order to make this goal attainable at a quantitative standard for application, absorptions of A band at high resolution have been undertaken by several authors [7–9], as above. Unfortunately, discrepancies of 15% in total band absorption intensity have been shown [7], and clearly much higher in individual lines. These difficulties had at the time only been ascribed to the closeness of rotational lines.

However, other limitations should be added as a possible source of uncertainty. In particular, absorption samplings of weak transitions in the gas phase obviously need the pressure, and/or the optical path, to be increased in order to get workable signals. Clearly, this makes the signal/noise ratio go often in the reverse direction, which is reflected in a loss of correlation among data.

A further drawback affecting oxygen's intensity data is that $b^1\Sigma_g^+ \leftarrow X^3\Sigma_g^-$ absorption happens to be strongly depleted for increasing pressure by $b^1\Sigma_g^+ \rightarrow a^1\Delta_g$ relaxation [23]. This, indeed, although forbidden for magnetic dipole by orbital selection rules, becomes allowed for electric dipole by collisions [17–20]. So, data on lines absorption intensity could be affected by unstable population, not to mention pressure-induced lineshifts [5].

Other remarkable questions, also stemming from the very long living dynamics between $b^1\Sigma_g^+$ and chemically active $a^1\Delta_g$, are studied by Raman and matrix-isolated configuration [20], at high pressures and in liquid phase with solvents [17–19], and in biochemistry [24,25] and medicine [26].

Such a variety of topics makes the availability of highly reliable data on A band structure a clear task for either fundamental [10,27,28] and applicative purposes. The linestrength structure shown here, as evaluated from the emission intensity of lines, is compared with theory as well as with reports from absorption experiments.

2. Experimental

In this laboratory [29], the intensity of forbidden emissons of diatomics has been observed in a rather traditional flowing afterglow apparatus, equipped with software control and counting chain. Many details have been reported elsewhere [30], therefore only a brief description of the experimental setup, with adopted methods, will be given in the following.

The equipment comprises cooled photomultipliers, a 1 m Czerny-Turner scanning monochromator with holographic grating, and a counts filter. Data collection is carried out by a software in multichannel analyzer configuration, with settings on scanning speed and sampling frequency matched to wavelength interval and aperture of slits (according to required FWHM for lines resolution). Software processing on acquired spectra allows the intensity of single lines to be readily obtained by a direct summation of their channel content.

In addition to shielding of microwave (μw) disturbances, maximum care is dedicated to the lowering and filtering of photomultiplier dark current, typically to values of a few counts/s. This is a crucial point for linestrength evaluation because of signal/noise ratio exponential decrease at high rotations. A pleasant consequence of this situation, on the other hand, is that no blur in linestrength, namely good self-correlation of deduced values, implies that negligible effects from noise are taking place (e.g., see Figs. 2–4). In plain words, no changes – i.e., no shifts – in the linestrength rotational dependence may be yielded by noise.

The oxygen $b^1\Sigma_g^+ \rightarrow X^3\Sigma_g^-$ long living ($\sim$11 s [13]) radiation is observed by μw excitation at 2450 MHz of controlled flowing admixtures with some rare gases – Ar, Ne, He – which allow the discharge to be stable for long scan durations ($\sim$1.5 h). The pumping speed is of 1800 l/min, with a residence time of about 1 s for gases in the cell. The emitting population is at room rotational temperature, owing to typical no gas rotational-translational heating from μw action.

Linestrengths are straightforwardly deduced by dividing the signal intensity of each line by its Boltzmann factor and radiation frequency power (see Section 4).

3. Results

In Fig. 1, the O_2 ($b^1\Sigma_g^+$ $v' = 0$–$X^3\Sigma_g^-$ $v'' = 0$) – or A band – emission is shown together with assignments. Only odd N values are present since $^{16}O_2$ antisymmetric rotational levels are missing because of zero nuclear spin [12].

It has to be pointed out that no difference in the spectrum profile is seen to arise by change of buffer gases (7–8 Torr) and/or oxygen pressure (0.1–0.2 Torr), apart from effects on the signal/noise ratio. The rotational branches are labeled in a $^{\Delta N}\Delta J$ form, J being the total angular momentum, and good [22,27] quantum number for rotational states in both Hund (a) and (b) cases [12,31], and N the angular momentum without spin

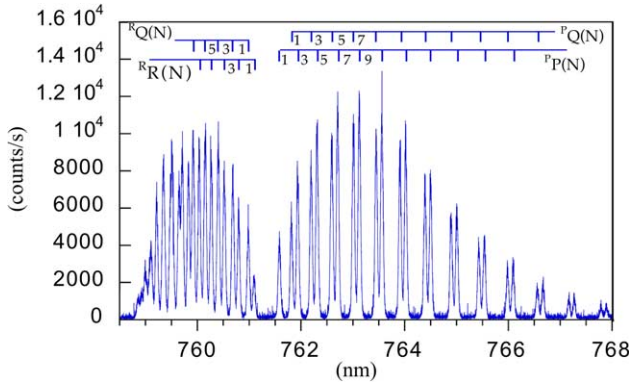

Fig. 1. The O_2 ($b^1\Sigma^+$ $v' = 0 \rightarrow {}^3\Sigma^-$ $v'' = 0$) emission (A band) from Ne (2.7 Torr) + He (5.0 Torr) + O_2 (0.1 Torr) microwave excitation. Resolution = 0.08 nm. N takes only odd values (see text).

($\mathbf{N} \equiv \mathbf{J} - \mathbf{S}$ in operator form), good quantum number for the Hund (b) case, which is featured by a weak spin coupling to the internuclear axis. The branches of ${}^1\Sigma_g^{\pm}$–${}^3\Sigma_g^{\mp}$ magnetic dipole transitions are of ^{R}R, ^{R}Q, ^{P}P and ^{P}Q type [10,12].

Figs. 2 and 3 have been evaluated from spectra obtained at different resolutions.

In Fig. 2, the linestrengths of ^{P}P and ^{P}Q branches are deduced from the spectrum reported in Fig. 1 (with FWHM of lines at 0.08 nm). Owing to good resolution of P wing "doublets" (see Fig. 1), the plot of Fig. 2 could have gone well beyond $J'' = 20$, however, data correlation is clearly seen to be increasingly hampered for $J'' > 13$ because of signal/noise ratio exponential decrease, as discussed in the previous section.

Values reported in Fig. 3 are from a better resolved spectrum of R wing, not shown, with FWHM of ^{R}R–^{R}Q lines at 0.06 nm.

In Fig. 4, the total linestrength structure is deduced from spectrum of Fig. 1. The cross-correlation between

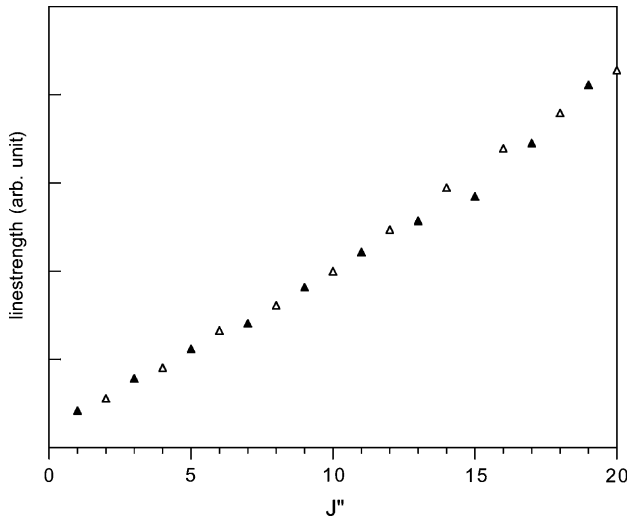

Fig. 2. The linestrength of ^{P}P and ^{P}Q branches. Values are deduced from spectrum shown in Fig. 1; ▲ (^{P}P); △ (^{P}Q).

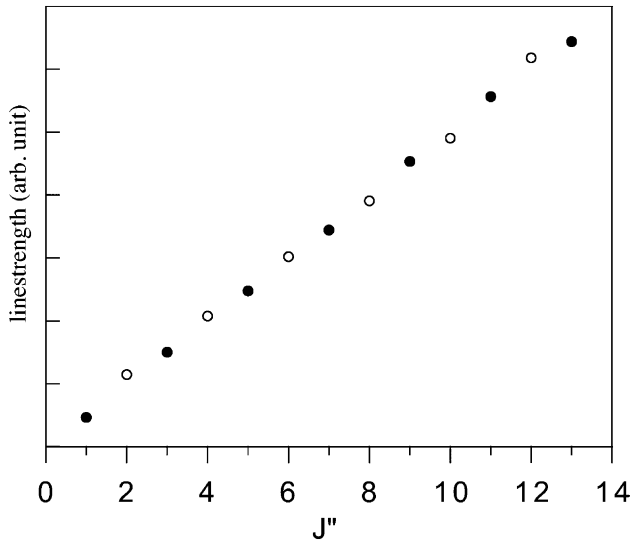

Fig. 3. The linestrength of ^{R}R and ^{R}Q branches. Values are deduced from a Ne (2.6 Torr) + He (5.0 Torr) + O_2 (≈0.1 Torr) spectrum of resolution = 0.06 nm, not shown; ● (^{R}R); ○ (^{R}Q).

P and R wings is more difficult to achieve, given that close noise conditions are easily lost in distant lines. So, only initial rotational lines are considered, with the low part of Fig. 2 reproduced.

The linestrength structure is expressed by the functional correlation existing among branches linestrength dependence on rotation, the experimental limit being thus given by self-correlation of linestrength deduced values.

The experimental limit is met at increasing rotation when the linestrength behavior is blurred by noise. Though blurred values are obviously of no use, in Fig. 2 the $J'' > 13$ sequence is reported to show this effect

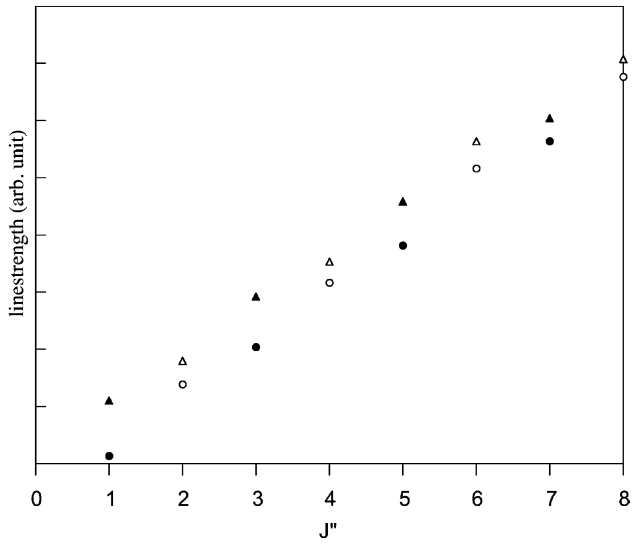

Fig. 4. The comprehensive linestrength correlation between ^{R}R, ^{R}Q, ^{P}P and ^{P}Q branches as deduced from spectrum shown in Fig. 1: ▲ (^{P}P); △ (^{P}Q); ● (^{R}R); ○ (^{R}Q).

Table 1
Signal intensity I of lines (no noise subtracted) and deduced linestrength l.s., with branches indication. Linestrengths are plotted in Fig. 4

J''	I (^{R}R)$\times 10^{-5}$ (counts/s)	l.s. (^{R}R) (arb. unit)	I (^{R}Q)$\times 10^{-5}$ (counts/s)	l.s. (^{R}Q) (arb. unit)	I (^{P}P)$\times 10^{-5}$ (counts/s)	l.s. (^{P}P) (arb. unit)	I (^{P}Q)$\times 10^{-5}$ (counts/s)	l.s. (^{P}Q) (arb. unit)
1	1.0922	1.1366			2.1049	2.1049		
2			2.2962	2.3888			2.6845	2.7963
3	2.6622	3.0375			3.7636	3.9223		
4			3.6515	4.1644			3.9587	4.5327
5	3.6508	4.8161			4.8776	5.5870		
6			4.6740	6.1597			5.0024	6.6395
7	4.1274	6.6363			5.2993	7.0369		
8			4.8314	7.7645			4.9764	8.0758

(which is also present in R wing for $J'' > 13$ and is not shown in Fig. 3).

Some brief comments on behaviors shown in the figures are given in the following:

Fig. 2: the ^{P}P (J) and ^{P}Q (J) linestrengths are unambiguously shown to follow the same function, which is not in agreement with the theoretical anticipation of a correlation $\Delta J'' = 1$ [10], or $\Delta J'' = 0.25$ [32], as used in the literature [7–9]. It has to be remembered here that widely known expressions of [10] are for $^{1}\Sigma^{\pm}$ lower state, and "reversed" expressions for the triplet state lower are easily deduced (e.g., can be found in [7]).

Fig. 3: once again, the linestrength of ^{R}R (J) and ^{R}Q (J) branches share the same function, at variance with theoretical prevision.

Fig. 4: the cross-correlation between R and P wings is reported, internal correlations being clearly in accord with Figs. 2 and 3. Here, the theoretical prevision of a $\Delta J'' = 1$ correlation [10,32] between ^{P}P (J) and ^{R}R (J) unperturbed branches is seen to hold. Although there is no substantial ambiguity in the R vs. P behavior of Fig. 4, a slightly worse data correlation, with respect to Figs. 2 and 3, is a typical effect of linestrength very high sensitivity to noise conditions. So, data reliability here is clearly shown by good correlations (and self-correlations) in Figs. 2–4.

The lines intensity I (in counts/s) is reported in Table 1 as obtained by software integration of the signal (see previous section) without noise subtraction, with deduced linestrengths (l.s.) (plotted in Fig. 4). The uncertainty is about 0.3%, according to $\sqrt{I}$ standard deviation.

4. Discussion

In the case of spontaneous emission, at thermal equilibrium in an isotropic medium, the radiation intensity distribution follows the law [12]

$$I(e'v'J';e''v''J'') \propto \nu_{J'J''}^{4} S_{J'J''} \exp[-F'(J')hc/kT], \tag{1}$$

where e and v labels are indicating electronic and vibrational states, respectively, and have been dropped on the right-hand side for clarity. In (1), $\nu_{J'J''}$ is the radiation frequency between upper ($'$) and lower ($''$) state, $S_{J'J''}$ the linestrength, and the $F'(J')$ term in the Boltzmann exponential factor the rotational energy of emitting level.

A general form for linestrength is [22,28,33]

$$S_{J'J''} = \Sigma_{M'M''} |\langle \Psi_{M'} | \mu | \Psi_{M''} \rangle|^2, \tag{2}$$

where μ is the total transition operator, depending on charge distribution, and ψ the wave function. Primed Ms indicate magnetic substates, here degenerate for no presence of external fields, not to be confused with magnetic dipole operator $\mathbf{M}$, which is the leading term in μ expression for this oxygen transition. Relations and units for magnetic dipole and electric dipole/quadrupole transitions can be found in [34].

In allowed transitions, and within the Born–Oppenheimer approximation, expression (2) essentially reduces to a single term of a well-known form, $q_{v'v''}R_{e}^{2}S_{J'J''}$, namely to a product of vibrational (Franck–Condon), electronic (squared transition moment), and rotational (Hönl–London) factors, respectively. In forbidden transitions, on the other hand, only terms of smaller magnitude survive, due to allowed contributions of higher orders from state perturbations [22,28] in the manifold. Furthermore, when μ is not appreciably affected during transition by changes occurring in the nuclear separation, like in this oxygen band, $q_{v'v''}$ can be dropped as a common factor.

One should be aware that the linestrength is linked in a very direct way to the wave function. Since, according to perturbation theory, a wave function approximated to the nth order involves energy up to the $(2n+1)$th order [35], this sensitivity is also reflected in the linestrength. The dependence of the latter on rotations is therefore a finer view of the structure of involved transition. Indeed, detailed aspects of transition may unequivocally show up [29] in linestrengths, while being hidden in lines position because of undistinguishable energy shifts. When a sufficient quantity of linestrength values is known (at least in two branches) for correlation, the complete rotational structure can be deduced [10,27,28]. In any case, such sensitivity should be effec-

tive in studies on weak transitions, where only higher order energy contributions may take place.

After pioneering works by Schlapp [32], and other classical literature centered on the oxygen molecule [36,37], a general and rigorous rationale for deduction of the linestrength dependence on rotation in forbidden transitions of diatomics has been described by Watson [10], with fundamental contributions by Hougen [27], and first applied to the $^3\Sigma$–$^1\Sigma$ simplest system.

Table I of Watson's paper, with all linestrengths only characterized by the perpendicular [10,13] component M of transition moment, can be readily specialized to the $^1\Sigma^{\pm}$–$^3\Sigma^{\mp}$ magnetic dipole transition. Branches distribution, following Watson's notations, are:

$$\begin{aligned}
&(F_2) \quad {}^{R}\mathrm{R}\ (\mathrm{J}) \propto J\ \mathrm{M}^2,\\
&(F_1) \quad {}^{R}\mathrm{Q}\ (\mathrm{J}) \propto s_{\mathrm{J}}^2(2J+1)\ \mathrm{M}^2,\\
&(F_2) \quad {}^{P}\mathrm{P}\ (\mathrm{J}) \propto (J+1)\ \mathrm{M}^2,\\
&(F_3) \quad {}^{P}\mathrm{Q}\ (\mathrm{J}) \propto c_{\mathrm{J}}^2(2J+1)\ \mathrm{M}^2,
\end{aligned} \tag{3}$$

where states are reversed with respect to Watson's Table I – i.e., here the triplet is lower – and with the provision that double primes are omitted. Involved fine structure terms F_i (J) ($i = 1$–3 at increasing energy) are also indicated. Expressions (3) also apply to absorption, and can be found for example in Ritter and Wilkerson [7].

In Hund (b) case, the fine structure terms are mixed by rotational perturbations, and a nearly linear dependence on the rotational quantum number is thus expected for linestrength. In equations above, c_{J} and s_{J} are the mixing coefficients of $^3\Sigma^-$ rotational terms, with general expressions

$$\begin{aligned}
&c_{\mathrm{J}}^2 = (F_2 - F_1)/(F_3 - F_1),\\
&s_{\mathrm{J}}^2 = (F_3 - F_2)/(F_3 - F_1).
\end{aligned} \tag{4}$$

It has to be emphasized here that (3) have been deduced using the Hund (a) case basis set on $^1\Sigma^+$ and $^3\Sigma^-$ effective [22] spin-rotation Hamiltonians, which are of the form for oxygen [10]

$$\begin{aligned}
&\mathrm{b}^1\Sigma_{\mathrm{g}}^+ \quad H' = B'J,\\
&\mathrm{X}^3\Sigma_{\mathrm{g}}^- \quad H = BN^2 + \gamma N\cdot S + 2\lambda S_z^2,
\end{aligned} \tag{5}$$

all constants being effective, and $\mathbf{N} \equiv \mathbf{J} - \mathbf{S}$. In (5), B' and B are the rotational constants (both $\cong 1.4$ cm^{-1}) [3], γ ($\cong -8.43 \times 10^{-3}$ cm^{-1}) [38] the spin-rotation coupling constant, and λ ($\cong 1.985$ cm^{-1}) [38] the fine structure parameter. Since state perturbations are less reflected into energies than into wave functions, as said above, Hamiltonian effective constants could be poorly affected by some state interactions. A direct consequence is for example that spin–orbit (s–o) and spin–spin (s–s) coupling energies are known to be undistinguishable by positional experiments, though states are differently contributing to the λ ($= \lambda_{\mathrm{so}} + \lambda_{\mathrm{ss}}$) effective value [22,38]. Because of these questions, a benchmark study on state-to-state spin interactions has been developed by an extended symmetry decomposition [39] of the NH manifold, which is identical to O_2, apart from the g/u labeling of homonuclear species. Owing to the character of calculations, results on symmetry should be applicable throughout to similar systems, and this may be of a great use for a detailed interpretation of linestrength behaviors in forbidden transitions.

General expressions (3) and (5) should be checked on experiment by comparing the observed linestrength dependence on rotations with adopted expressions of c_{J} and s_{J} coefficients.

If λ is small with respect to B, or at high rotations, Watson's eigenvalues of $\mathrm{X}^3\Sigma_{\mathrm{g}}^-$ effective Hamiltonian (5) can be approximated, and the rotational dependence of fine structure levels takes a convenient form [10] (double primes omitted):

$$\begin{aligned}
&F_1(J) = F_2(J) - \lambda + \lambda/(2J+1) - (2B-\gamma)J,\\
&F_2(J) = BJ(J+1) + 2\lambda - \gamma,\\
&F_3(J) = F_2(J) - \lambda - \lambda/(2J+1) + (2B-\gamma)(J+1),
\end{aligned} \tag{6}$$

$F_2(J)$ being the unperturbed term. So, when λ terms happen to be negligible, the Watson perturbation coefficients are readily deduced from (4)

$$c_{\mathrm{J}}^2 = J/(2J+1); \quad s_{\mathrm{J}}^2 = (J+1)/(2J+1). \tag{7}$$

If this is the case, by substitution in (3) the expected linestrength behaviors would be

$$\begin{aligned}
&(F_2) \quad {}^{R}\mathrm{R}\ (\mathrm{J}) \propto J\ \mathrm{M}^2,\\
&(F_1) \quad {}^{R}\mathrm{Q}\ (\mathrm{J}) \propto (J+1)\ \mathrm{M}^2,\\
&(F_2) \quad {}^{P}\mathrm{P}\ (\mathrm{J}) \propto (J+1)\ \mathrm{M}^2\\
&(F_3) \quad {}^{P}\mathrm{Q}\ (\mathrm{J}) \propto J\ \mathrm{M}^2.
\end{aligned} \tag{8}$$

Consequently, both ^{R}R (J)–^{R}Q (J) and ^{P}Q (J)–^{P}P (J) "doublets" (see Fig. 1) would exhibit a shift of one J unit, with ^{R}R–^{P}Q and ^{R}Q–^{P}P superposed.

In [7], with many others ([9, and references therein]), the foreseen linestrength behavior is centered on Watson's treatment. Reported functions for perturbed branches are ^{P}Q (J) $\propto [J + \lambda/(2B-\gamma)]$ and ^{R}Q (J) $\propto [J + 1 - \lambda/(2B-\gamma)]$, where the adopted coefficients $c_{\mathrm{J}}^2 = [J + \lambda/(2B-\gamma)]/(2J+1)$ and $s_{\mathrm{J}}^2 = [J + 1 - \lambda/(2B-\gamma)]/(2J+1)$ [40] are still in the small λ approximation at low rotations, and different from (7) by merely keeping $-\lambda$ in perturbed $F_1(J)$ and $F_3(J)$ terms of (6). Accordingly, and owing to O_2 constants reported above, the theoretical prediction is close to: ^{P}Q (J) $\propto (J + 0.7)$ and ^{R}Q (J) $\propto (J + 0.3)$, with ^{P}P (J) and ^{R}R (J) as in (3). Therefore, ^{P}Q (J) and ^{R}Q (J) linestrengths are expected to be reciprocally shifted by some 1/3 of rotational J unit within ^{P}P (J) and ^{R}R (J) limits, which are shifted by one J unit. In other words, linestrength rotational dependence of ^{R}R (J)–^{R}Q (J)–^{P}Q (J)–^{P}P (J) branches are expected to be about equally spaced in this order,

spanning one J unit. In [7], data have been found in agreement within experimental errors, and this is also confirmed in more recent works [9].

In [8], the Schlapp expressions, closely resembling those above, $^{P}P\ (J) \propto (J+1)\ M^2$, $^{P}Q\ (J) \propto (J+0.75)\ M^2$, $^{R}R\ (J) \propto J\ M^2$ and $^{R}Q\ (J) \propto (J+0.25)\ M^2$ are taken as valid.

For an interpretation of the unexpected behaviors of Figs. 2–4) it is necessary, first of all, to find out c_J and s_J expressions which are fitting the experiment. Actually, (6) are polynomial approximations of Hamiltonian's triplet eigenvalues [10,27], in order to describe a nearly linear dependence of shifts on rotational perturbation. However, the Breit–Pauli Hamiltonian H_{BP} comprise [39] both s–o and s–s couplings, and the occurrence of $\lambda_{BP} > B$ in O_2 appears to prevent the applicability of the small λ approximation (6). If the state perturbation $b^1\Sigma_g^+ \sim X^3\Sigma_{g0}^-$ is considered, on the other hand, it is seen that it contributes about 99% [38,41] of total spin–orbit interactions, and no s–s (<s–o in oxygen [13,38]). A reduction of the effective Hamiltonian H_{BP} to H_{so} for the triplet in O_2 (b–X) transition could make approximations (6) to become somehow acceptable because of a smaller fine structure constant [38] $\lambda_{so} \approx 1.240\ cm^{-1}$.

However, a stronger argument is that only the $b^1\Sigma_g^+$–$X^3\Sigma_{g\pm1}^-$ perpendicular share of the transition [10,13] can be present here. Since the fine structure width is obviously defined by both $X^3\Sigma_{g0}^-$ and $X^3\Sigma_{g\pm1}^-$ levels, this circumstance should imply λ_{BP} to be immaterial for transition mechanisms. Good linestrength linearity from initial values in Figs. 2–4 is also apparent, and seems to exclude λ presence. A previous study [42] on the isoelectronic NF molecule, on the other hand, has shown the ($b^1\Sigma^+$–$X^3\Sigma^-$) linestrength correlations to be strongly affected by s–s ($\gg$s–o) coupling, though not involved in transition mechanisms. In electric dipole transitions, in other words, all λ couplings may happen to be reflected into linestrength, probably because all fine structure limiting states are involved by both the presence of the parallel and the perpendicular component.

According to above, with $\lambda = 0$ in (6), Watson's coefficients (7) with related linestrength expressions (8) should apply. As shown a few years ago [43], however, the Hund (b) case can take place in two configurations, that have been distinguished as an intermediate (a)–(b) and a full (b) case. Both have been shown to occur, divided by a flat intermediate phase, in the linestrength distribution of either PH and PD [43,44] radicals. Given explanation has been that of $J \to N$ transition in the rotational good quantum number, referring to the variable which identifies the rotational state of a multiplet. In [10,40], on the contrary, coefficients (7), and those in [7] reported above, are, respectively, defined of limiting Hund (b) case and close to limit. This seems not to be the case in my opinion, because these coefficients are characterized by the good quantum number J, which is well defined in both (a) and (b) cases [22,27], and thus should also be in the intermediate (a)–(b) case, where N is not well defined because of an incomplete spin decoupling [12] from the nuclear axis. The latter assertion comes from energy levels expressions (6), where the fine structure is depending on molecular constant B.

Formulas of the full (b) case, on the other hand, are deduced [43] by fixing terms of N triplets with a straightforward application of $J \Longleftrightarrow N$ correspondences $J = N+1$, N and $N-1$ to F_1, F_2 and F_3 terms, respectively [12]. From (6) with $\lambda = 0$, the new term functionals for the transition are given by $F_1(N) = F_2(N) + \gamma(N+1)$, $F_2(N) = BN(N+1) - \gamma$ and $F_3(N) = F_2(N) - \gamma N$. Apart from λ, the lack of B constant in the fine structure shows that a spin coupling transition from the molecular internuclear axis to a rotational axis has been completed. In other words, the molecular structure is "forgotten" in spin precession energy terms, now only depending on γ. Related coefficients $c_N^2 = (N+1)/(2N+1)$ and $s_N^2 = N/(2N+1)$ are easily obtained from (4) [43]. The N label of coefficients is to underline that splittings here are referred to triplets which are N single valued, whatever the rotational variable in formulas. Expressions (3) after $J \Longleftrightarrow N$ conversion become: $F_2)$ $^{R}R(N) \propto N\ M^2$; $F_1)$ $^{R}Q(N) \propto s_{N+1}^2(2N+3)\ M^2$; $F_2)$ $^{P}P(N) \propto (N+1)\ M^2$ and $F_3)$ $^{P}Q(N) \propto c_{N-1}^2(2N-1)\ M^2$.

Substitution of coefficients gives the full Hund (b) case linestrength dependence on rotation which, again from $J \Longleftrightarrow N$ correspondences, can be expressed in both variables:

$$\begin{aligned} &(F_2) \quad {}^{R}R \propto N\ M^2 = J\ M^2, \\ &(F_1) \quad {}^{R}Q \propto (N+1)\ M^2 = J\ M^2, \\ &(F_2) \quad {}^{P}P \propto (N+1)\ M^2 = (J+1)\ M^2, \\ &(F_3) \quad {}^{P}Q \propto N\ M^2 = (J+1)\ M^2. \end{aligned} \tag{9}$$

The functions of perturbed ^{R}Q and ^{P}Q branches are thus "exchanged" with respect to (8) by typical [43,44] values of c and s coefficients for the full (b) case. This is in good agreement with findings shown in Figs. 2–4. It seems reasonable, on the other hand, that the Hund full (b) case takes place when the fine structure magnitude is not influential. Clearly, however, further experiments on the magnetic dipole linestrength of forbidden transitions are desirable.

5. Conclusions

Basics results from experiments on a widely known forbidden transition of the oxygen molecule have been given. The method used is that of Quantitative Spectroscopy (i.e., intensity of lines), which is a dual view with respect to Positional Spectroscopy (i.e., lines position in the energy scale). Data are lacking in this area,

though clearly helpful in such different realms as atmospheric monitoring, modelings and other applications. These quantitative techniques now allow observations on diatomics and, together with extensions of the theory as outlined here, may permit a satisfactory interpretation of available data.

References

[1] H.I. Shiff, Aeronomy of the stratosphere and mesosphere International Association of Geomagnetism and Aeronomy. Symposium (Kioto, Japan); Can. J. Chem. 52 (1974) 1381.
[2] R. Hernández-Lamoneda, M.I. Hernandez, J. Campos-Martínez, Chem. Phys. Lett. 368 (2003) 709.
[3] P.H. Krupenie, J. Phys. Chem. Ref. Data 1 (1972) 423.
[4] H.D. Babcock, L. Herzberg, Astrophys. J. 108 (1948) 167.
[5] A.J. Phillips, A.J. Peters, P.A. Hamilton, J. Mol. Spectrosc. 184 (1997) 162.
[6] R.N. Zare, in: K. Naharari Rao, C.W. Mathews (Eds.), Molecular Spectroscopy: Modern Research, Academic Press, New York, 1972, p. 207.
[7] K.J. Ritter, T.D. Wilkerson, J. Mol. Spectrosc. 121 (1987) 1.
[8] T. Nakazawa, T. Yamanouchi, M. Tanaka, J. Quantum Spectrosc. Radiat. Transfer 27 (1982) 615.
[9] L.R. Brown, C. Plymate, J. Mol. Spectrosc. 199 (2000) 166.
[10] J.K.G. Watson, Can. J. Phys. 46 (1968) 1637.
[11] T.G. Slanger, P.C. Cosby, Phys. Chem. 92 (1988) 267.
[12] G. Herzberg, Molecular Specra and Molecular Structure: Spectra of Diatomic Molecules, Van Nostrand, Princeton, NJ, 1950.
[13] B. Minaev, O. Vahtras, H. Agren, Chem. Phys. 208 (1996) 299.
[14] L. Wallace, J.W. Chamberlain, Planet. Space Sci. 2 (1958) 60.
[15] M.R. Torr, D.G. Torr, R.R. Laher, J. Geophys. Res. 90 (1985) 8525.
[16] R.L. Gattinger, A.J. Vallance-Jones, J. Geophys. Res. 81 (1976) 4789.
[17] B.F. Minaev, H. Agren, J. Chem. Soc., Faraday Trans. 93 (1997) 2231.
[18] C. Long, D.R. Kearns, J. Chem. Phys. 59 (1973) 5729.
[19] R. Schmidt, M. Bodesheim, J. Phys. Chem. 99 (1995) 15919.
[20] G. Tyczkowski, U. Schurath, M. Bodenbinder, H. Willner, Chem. Phys. 215 (1997) 379.
[21] C.L. Korb, C.Y. Weng, Appl. Opt. 22 (1983) 3759.
[22] H. Lefebvre-Brion, R.W. Field, Perturbations in the Spectra of Diatomic Molecules, Academic Press, New York, 1986.
[23] J.F. Noxon, Can. J. Phys. 39 (1961) 1110.
[24] C.S. Foote, in: W.A. Pryor (Ed.), Free Radicals in Biology, vol. 2, Academic Press, New York, 1976.
[25] D. Gal, Biochem. Biophys. Res. Commun. 202 (1994) 10.
[26] Y. Li, M.A. Trush, Cancer Res. 54 (Suppl.) (1994) 1895s.
[27] J.T. Hougen, The Calculation of Rotational Energy Levels and Rotational Line Intensities in Diatomic Molecules, Natl. Bur. Std. (US) Monogr. 115, 1970.
[28] E.E. Whiting, R.W. Nicholls, Astrophys. J. Suppl. Series 27 (1974) 1.
[29] G. Di Stefano, Trends Chem. Phys. 10 (2002) 63.
[30] G. Di Stefano, A. Ricci, Appl. Spectrosc. 11 (1993) 1788.
[31] G. Herzberg, The Spectra and Structures of Simple Free Radicals, Cornell University Press, Ithaca, 1971.
[32] R. Schlapp, Phys. Rev. 51 (1937) 342.
[33] E.E. Whiting, A. Schadee, J.B. Tatum, J.T. Hougen, R.W. Nicholls, J. Mol. Spectrosc. 80 (1980) 249.
[34] J.B. Tatum, The Interpretation of Intensities in Diatomic Molecular Spectra, Astrophys. J. Suppl. Series XVI (1967) 21.
[35] P.O. Löwdin, J. Mol. Spectrosc. 13 (1964) 326.
[36] M. Tinkham, W.P. Strandberg, Phys. Rev. 97 (1955) 937.
[37] K. Kayama, J.C. Baird, J. Chem. Phys. 46 (1967) 2604.
[38] F.D. Waine, E.A. Colbourn, Mol. Phys. 34 (1977) 1141.
[39] D.R. Yarkony, J. Chem. Phys. 91 (1989) 4745.
[40] J.B. Tatum, J.K.G. Watson, Can. J. Phys. 49 (1971) 2693.
[41] R. Klotz, C.M. Marian, S.D. Peyerimhoff, B.A. Hess, R. Buenker, J. Chem. Phys. 89 (1984) 223.
[42] G. Di Stefano, M. Lenzi, G. Piciacchia, A. Ricci, J. Chem. Phys. 107 (1997) 2752.
[43] G. Di Stefano, M. Lenzi, G. Piciacchia, A. Ricci, Chem. Phys. 165 (1992) 201.
[44] G. Di Stefano, M. Lenzi, A. Ricci, Chem. Phys. 246 (1999) 267.